be determined at this point:

$$n = \frac{M_1 - m}{T_1 e^{-\gamma l_1}} = \frac{M_2 - m}{T_2 e^{-\gamma l_2}} \tag{8}$$

$$t = \sqrt{\frac{T_1(1 - n^2 e^{-2\gamma l_1})}{e^{-\gamma l_1}}} = \sqrt{\frac{T_2(1 - n^2 e^{-2\gamma l_2})}{e^{-\gamma l_2}}}. \tag{9}$$

Some precautions are necessary, in particular, those due to the determination of m. The relation obtained (6) contains several subtractions, both in the numerator and the denominator. This calculation is very sensitive to experimental errors; hence, the utmost care is needed during measurements. One possible way to avoid this delicate step is to determine m directly, which can be done by introducing the tip of a lossy termination inside of the loaded waveguide section [Fig. 8(c)], in which case $h \rightarrow 0$ and $M = m$. Of course, this can only be done with rather thin slabs.

ACKNOWLEDGMENT

The authors wish to thank Dr. M. S. Ramachandraiah and R. Cabi-Akman for their help in the experimental part of this project. All the calculations were carried out at the Computation Center of the Ecole Polytechnique Fédérale.

REFERENCES

[1] V. R. Bui and R. R. J. Gagné, "Dielectric losses in an H-plane-loaded rectangular waveguide," *IEEE Trans. Microwave Theory Tech.* (Short Papers), vol. MTT-20, pp. 621–623, Sept. 1972.
[2] R. M. Arnold and F. J. Rosenbaum, "Nonreciprocal wave propagation in semiconductor loaded waveguides in the presence of a transverse magnetic field," *IEEE Trans. Microwave Theory Tech.*, vol. MTT-19, pp. 57–65, Jan. 1971.
[3] R. Collin, *Field Theory of Guided Waves.* New York: McGraw-Hill, 1960, ch. 6.
[4] F. E. Gardiol, "Higher-order modes in dielectrically loaded rectangular waveguides," *IEEE Trans. Microwave Theory Tech.*, vol. MTT-16, pp. 919–924, Nov. 1968.
[5] F. E. Gardiol and A. S. Vander Vorst, "Wave propagation in a rectangular waveguide loaded with an H-plane dielectric slab," *IEEE Trans. Microwave Theory Tech.* (Corresp.), vol. MTT-17, pp. 56–57, Jan. 1969.
[6] F. E. Gardiol, "Anisotropic slabs in rectangular waveguides," *IEEE Trans. Microwave Theory Tech.*, vol. MTT-18, pp. 461–467, Aug. 1970.
[7] H. R. Witt, R. E. Biss, and E. L. Price, "Propagation constants of a waveguide containing parallel sheets of finite conductivity," *IEEE Trans. Microwave Theory Tech.*, vol. MTT-15, pp. 232–239, Apr. 1967.
[8] L. B. Felsen, "Representation and measurement of reciprocal discontinuity structures in single mode waveguide," in *Handbook of Microwave Measurements*, M. Sucher and J. Fox, Eds. Brooklyn, N. Y.: Polytech. Press of Polytech. Inst. Brooklyn, 1963, ch. IV.
[9] P. Delogne, "Compensation à l'aide d'un ordinateur des mesures des paramètres d'un quadripôle aux hyperfréquences," *Rev. HF (Brussels)*, vol. 8, July 1968.
[10] S. Ramo, J. R. Whinnery, and T. Van Duzer, *Fields and Waves in Communication Electronics.* New York: Wiley, 1967, p. 378.

Analysis of Thick Rectangular Waveguide Windows With Finite Conductivity

RAYMOND J. LUEBBERS AND BENEDIKT A. MUNK

***Abstract*—The modal analysis method is used to calculate the reflection and transmission properties of a thick rectangular window centrally located in a rectangular waveguide. Excellent agreement is obtained between calculated and measured values for windows of intermediate thickness. For thicker windows made of finitely conducting materials, the results obtained using perfectly conducting waveguide modes are inaccurate. However, by modifying the modes so as to include some of the mode-coupling effects caused by the surface currents, good agreement between calculated and measured data is obtained for a very thick, finitely conducting window.**

Manuscript received September 17, 1972; revised January 24, 1973. This work was supported in part by Contract F33615-70-C-1439 between Air Force Avionics Laboratory, Air Force Systems Command, Wright-Patterson Air Force Base, Ohio, and The Ohio State University Research Foundation.

The authors are with the ElectroScience Laboratory, Department of Electrical Engineering, The Ohio State University, Columbus, Ohio 43212.

INTRODUCTION

IN THIS PAPER we are concerned with calculating the reflection and transmission properties of a thick, finitely conducting rectangular resonant window in a rectangular waveguide. The geometry of the problem and the coordinate system used are shown in Fig. 1. The window is assumed to be centered in the waveguide with the energy propagating in the z direction.

If the slot is infinitesimally thin, i.e., $l \rightarrow 0$, variational techniques can be used to obtain an expression for the equivalent shunt impedance from which the reflection and transmission coefficients can be calculated [1, pp. 88–97]. For finite values of l, however, this method appears to be very difficult to apply, except for the degenerate cases where the slot width equals the waveguide width (capacitive obstacle) or the slot height equals the waveguide height (inductive obstacle). Results for these cases are given by Marcuvitz [2].

The approach used in this paper is based on the modal analysis method of Wexler [3]. This is a general method that can be applied to a broad class of waveguide discontinuity problems. In his paper, Wexler performed calculations for a perfectly conducting two-dimensional obstacle, and compared his results (with good agreement) to results given in Marcuvitz. In this paper, modal analysis is used to analyze a three-dimensional obstacle, and the results are compared with measurements. Good agreement is obtained for resonant windows of intermediate thickness ($0 < l/\lambda < 0.1$) using perfectly conducting waveguide modes to represent the fields in the window.

However, for a thick ($l \approx \lambda$), narrow ($h \ll t$), finitely conducting (brass) resonant window, the results obtained using modal analysis do not yield such good agreement with measurements. However, by modifying the propagation constant of the waveguide modes used to represent the fields in the window so as to include the mode coupling due to surface currents, a significant improvement in accuracy is obtained.

Perfectly Conducting Waveguide Window

In order to apply the modal analysis method, we consider our rectangular window to be a small waveguide, denoted as region b in Fig. 1, while the large waveguide is denoted as region a. The problem is now treated as a waveguide junction problem. The transverse components of the modes in region a are [1, p. 21]

$$e_{ai} = u_x \sin\left(\frac{p\pi y}{w}\right) \cos\left(\frac{q\pi x}{v}\right) \tag{1}$$

$$h_{ai} = u_y y_{ai} \sin\left(\frac{p\pi y}{w}\right) \cos\left(\frac{q\pi x}{v}\right) - u_x\sqrt{-1}\sqrt{\frac{\epsilon}{\mu}}\,\frac{\lambda}{2\pi} \cdot \frac{\dfrac{pq\pi^2}{wv}}{\sqrt{\left(\dfrac{p\pi}{w}\right)^2 + \left(\dfrac{q\pi}{v}\right)^2 - \left(\dfrac{2\pi}{\lambda}\right)^2}} \cdot \cos\left(\frac{p\pi y}{w}\right) \sin\left(\frac{q\pi x}{v}\right) \tag{2}$$

where u_x and u_y are unit vectors, p and q are the conventional mode numbers, and y_{ai} is the wave admittance of the ith mode given by

$$y_{ai} = \sqrt{-1}\sqrt{\frac{\epsilon}{\mu}}\,\frac{\lambda}{2\pi} \cdot \frac{\left(\dfrac{2\pi}{\lambda}\right)^2 - \left(\dfrac{p\pi}{w}\right)^2}{\sqrt{\left(\dfrac{p\pi}{w}\right)^2 + \left(\dfrac{q\pi}{v}\right)^2 - \left(\dfrac{2\pi}{\lambda}\right)^2}}. \tag{3}$$

Similarly, in region b [i.e., $(w-t)/2 < y < (w+t)/2$ and $(v-h)/2 < x < (v+h)/2$], the transverse components of the modes are

$$e_{bj} = u_x \sin\left(r\pi\cdot\frac{2y - w + t}{2t}\right) \cos\left(s\pi\cdot\frac{2x - v + h}{2h}\right) \tag{4}$$

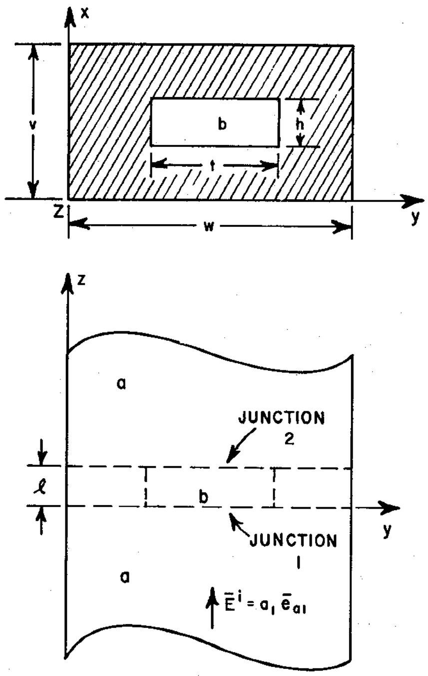

Fig. 1. Geometry and coordinate system for a thick rectangular slot in a rectangular waveguide.

$$h_{bj} = u_y y_{bj} \sin\left(r\pi\cdot\frac{2y - w + t}{2t}\right) \cdot \cos\left(s\pi\cdot\frac{2x - v + h}{2h}\right) - u_x\sqrt{-1}\sqrt{\frac{\epsilon}{\mu}}\,\frac{\lambda}{2\pi} \cdot \frac{\dfrac{rs\pi^2}{th}}{\sqrt{\left(\dfrac{r\pi}{t}\right)^2 + \left(\dfrac{s\pi}{h}\right)^2 - \left(\dfrac{2\pi}{\lambda}\right)^2}} \cdot \cos\left(r\pi\cdot\frac{2y - w + t}{2t}\right) \sin\left(s\pi\cdot\frac{2x - v + h}{2h}\right) \tag{5}$$

where r and s are the mode numbers and y_{bj} is given by

$$y_{bj} = \sqrt{-1}\sqrt{\frac{\epsilon}{\mu}}\,\frac{\lambda}{2\pi} \cdot \frac{\left(\dfrac{2\pi}{\lambda}\right)^2 - \left(\dfrac{r\pi}{t}\right)^2}{\sqrt{\left(\dfrac{r\pi}{t}\right)^2 + \left(\dfrac{s\pi}{h}\right)^2 - \left(\dfrac{2\pi}{\lambda}\right)^2}}. \tag{6}$$

These modes are neither TE nor TM, but are characterized by the absence of a y-directed E field. Modes are numbered consecutively, i.e., $i = 1, 2, 3, \cdots$, and $j = 1, 2, 3, \cdots$, where each value of i corresponds to particular values for p and q, etc. Due to symmetry, not all modes are excited; p and r are always odd, q and s are even (or 0) for this geometry and excitation.

Consider the mode $i = 1$ with strength a_1 emanating from a matched source in waveguide a and impinging on waveguide

b (the slot) at junction 1 (see Fig. 1). Taking $\boldsymbol{E}$ to be the total transverse electric field at the discontinuity, the field expanded in terms of modes just below junction 1 is

$$\boldsymbol{E} = (1+\rho)a_1\boldsymbol{e}_{a1} + \sum_{i=2}^{\infty} a_i\boldsymbol{e}_{ai} \tag{7}$$

where ρ is the reflection coefficient for mode $i=1$, and the a_i are the coefficients of the backscattered modes. The total transverse magnetic field $\boldsymbol{H}$ is expressed by

$$\boldsymbol{H} = (1-\rho)a_1\boldsymbol{h}_{a1} - \sum_{i=2}^{\infty} a_i\boldsymbol{h}_{ai}. \tag{8}$$

Referring again to Fig. 1, the fields in waveguide b just above junction 1 are to be expressed in terms of modes in b. However, one must account for the reflection of these modes from junction 2, since each transmitted mode j reaching junction 2 will scatter power into other modes k, some of which return to junction 1. It is therefore necessary to account for these returned waves, as well as for the positively directed ones, when summing modes. In order to do this, a scattering coefficient S_{jk} is defined as equal to the mode coefficient b_k of the kth backscattered mode present just above junction 1 due to mode j scattering from junction 2. Clearly, to find the fields due to one wave incident on the slot, junction 2 must be solved for each j mode. These tedious computations can be avoided for this problem since the obstacle is symmetric about the $z=l/2$ plane. By using symmetric and antisymmetric excitations, we can find the T-equivalent circuit parameters without evaluating a complete set of scattering coefficients. Symmetric excitation of the slot is obtained by having two modes in the waveguide, one traveling in the $+z$ direction and the other in the $-z$ direction, such that the E fields are in phase in the $z=l/2$ plane; antisymmetric excitation is obtained if these modes are 180° out of phase. For symmetric excitation, an open circuit appears at the symmetry plane; antisymmetrical excitation produces a short circuit. Under these conditions, $S_{jk}=0$ for $j\neq k$, and

$$S_{jj} = \pm e^{-\Gamma_j l} \tag{9}$$

where Γ_j is the propagation constant for mode j in guide b. For a rectangular slot with modes as defined previously [(4)–(6)]

$$\Gamma_j = \sqrt{\left(\frac{r\pi}{t}\right)^2 + \left(\frac{s\pi}{h}\right)^2 - \left(\frac{2\pi}{\lambda}\right)^2}. \tag{10}$$

The plus and minus signs in (9) correspond to symmetrical and antisymmetrical excitation, respectively. With antisymmetrical excitation, the computed input impedance of the window is equal to the upper arm impedance Z_m of the equivalent T circuit, so that

$$\frac{Z_m}{Z_{\text{wg}}} = \frac{1+\rho_a}{1-\rho_a} \tag{11}$$

where ρ_a is the dominant mode reflection coefficient [see (7)] with antisymmetric excitation and Z_{wg} is the waveguide impedance. The common branch impedance Z_{12} can be found from the above equation and from the fact that for symmetrical excitation we have

$$\frac{Z_m + 2Z_{12}}{Z_{\text{wg}}} = \frac{1+\rho_s}{1-\rho_s} \tag{12}$$

with ρ_s the reflection coefficient for symmetric excitation.

With either symmetric or antisymmetric excitation, the fields in region b just above junction 1 are given by

$$\boldsymbol{E} = \sum_{j=1}^{\infty} b_j\boldsymbol{e}_{bj}(1+S_{jj}) \tag{13}$$

$$\boldsymbol{H} = \sum_{j=1}^{\infty} b_j\boldsymbol{h}_{bj}(1-S_{jj}) \tag{14}$$

where b_j is the coefficient of the jth mode.

To solve for the unknown coefficient ρ, the boundary conditions at the discontinuity must be satisfied: continuity of transverse electric and magnetic fields across the aperture, and zero tangential $\boldsymbol{E}$ at the surface which contains the window.

In waveguide region a [4, p. 230]

$$\int_a \boldsymbol{e}_{ai} \times \boldsymbol{h}_{am}\cdot\boldsymbol{u}_z\, ds = 0 \tag{15}$$

where m is a mode number in waveguide a, $i\neq m$, and $\int_a ds$ denotes an integration over the cross section of waveguide a. Following Wexler's procedure, we enforce continuity of transverse electric field at junction 1 by equating (7) with (13), taking the cross product with $\boldsymbol{h}_{am}$, and integrating, keeping in mind the orthogonality relation of (15). The results are

$$(1+\rho)a_1\int_a \boldsymbol{e}_{a1}\times\boldsymbol{h}_{a1}\cdot\boldsymbol{u}_z\, ds = \sum_{j=1}^{\infty} b_j\int_b \boldsymbol{e}_{bj}\times\boldsymbol{h}_{a1}\cdot\boldsymbol{u}_z\, ds\cdot(1+S_{jj}) \tag{16}$$

for $m=1$ and

$$a_m\int_a \boldsymbol{e}_{am}\times\boldsymbol{h}_{am}\cdot\boldsymbol{u}_z\, ds = \sum_{j=1}^{\infty} b_j\int_b \boldsymbol{e}_{bj}\times\boldsymbol{h}_{am}\cdot\boldsymbol{u}_z\, ds\cdot(1+S_{jj}) \tag{17}$$

for $m\neq 1$, where $\int_b ds$ denotes an integration over the cross section of waveguide b.

To provide continuity of the transverse magnetic field through the aperture, we equate (8) and (14), take a cross product with $\boldsymbol{e}_{bn}$, and integrate. By using the orthogonality relation

$$\int_b \boldsymbol{e}_{bn}\times\boldsymbol{h}_{bj}\cdot\boldsymbol{u}_z\, ds = 0 \tag{18}$$

the result is

$$(1-\rho)a_1\int_b \boldsymbol{e}_{bn}\times\boldsymbol{h}_{a1}\cdot\boldsymbol{u}_z\, ds - \sum_{i=2}^{\infty} a_i\int_b \boldsymbol{e}_{bn}\times\boldsymbol{h}_{ai}\cdot\boldsymbol{u}_z\, ds = b_n(1-S_{nn})\int_b \boldsymbol{e}_{bn}\times\boldsymbol{h}_{bn}\cdot\boldsymbol{u}_z\, ds. \tag{19}$$

If we now substitute (17) into (19) and change index m to i, the a_i coefficients are eliminated, and we obtain the equation

$$\rho \int_b \boldsymbol{e}_{bn} \times \boldsymbol{h}_{a1} \cdot \boldsymbol{u}_z \, ds + \sum_{j=1}^{N} \frac{b_j}{a_1} \sum_{i=2}^{M} \frac{\int_b \boldsymbol{e}_{bj} \times \boldsymbol{h}_{ai} \cdot \boldsymbol{u}_z \, ds (1 + S_{jj})}{\int_a \boldsymbol{e}_{ai} \times \boldsymbol{h}_{ai} \cdot \boldsymbol{u}_z \, ds} \cdot \int_b \boldsymbol{e}_{bn} \times \boldsymbol{h}_{a1} \cdot \boldsymbol{u}_z \, ds + \frac{bn}{a_1} (1 - S_{nn}) \int_b \boldsymbol{e}_{bn} \times \boldsymbol{h}_{bn} \cdot \boldsymbol{u}_z \, ds = \int_b \boldsymbol{e}_{bn} \times \boldsymbol{h}_{a1} \cdot \boldsymbol{u}_z \, ds. \tag{20}$$

Since the computer can solve only a limited number of equations, the infinite series were truncated at M and N, where M and N are the number of modes used to approximate the fields in waveguide regions a and b, respectively. Equation (20) is really N linear equations corresponding to $n = 1, 2, 3, \cdots, N$. There are $N+1$ unknowns, namely, ρ and the N modal coefficients in waveguide $b((b_1/a_1), (b_2/a_1), \cdots, (b_N/a_1))$, but by dividing (16) by a_1 and rearranging, we have

$$\rho \int_a \boldsymbol{e}_{a1} \times \boldsymbol{h}_{a1} \cdot \boldsymbol{u}_z \, ds - \sum_{j=1}^{N} \frac{b_j}{a_1} (1 + S_{jj}) \int_b \boldsymbol{e}_{bj} \times \boldsymbol{h}_{ai} \cdot \boldsymbol{u}_z \, ds = - \int_a \boldsymbol{e}_{a1} \times \boldsymbol{h}_{a1} \cdot \boldsymbol{u}_z \, ds \tag{21}$$

which, in combination with (20), forms a system of $N+1$ linear equations with $N+1$ unknowns.

The integrations are fairly straightforward for this problem, and are as follows:

$$\int_a \boldsymbol{e}_{ai} \times \boldsymbol{h}_{ai} \cdot \boldsymbol{u}_z \, ds = y_{ai} \int_0^w \int_0^v \sin^2 \left(\frac{p\pi y}{w} \right) \cos^2 \left(\frac{q\pi x}{v} \right) dx \, dy = \begin{cases} 0.25 \, wv \, y_{ai}, & \text{if } q \neq 0 \\ 0.50 \, wv \, y_{ai}, & \text{if } q = 0 \end{cases} \tag{22}$$

$$\int_b \boldsymbol{e}_{bj} \times \boldsymbol{h}_{bj} \cdot \boldsymbol{u}_z \, ds = y_{bj} \int_{(w-t)/2}^{(w+t)/2} \int_{(v-h)/2}^{(v+h)/2} \sin^2 \left(r\pi \cdot \frac{2y - w + t}{2t} \right) \cdot \cos^2 \left(s\pi \cdot \frac{2x - v + h}{2h} \right) dx \, dy = \begin{cases} 0.25 \, th \, y_{bj}, & \text{if } s \neq 0 \\ 0.50 \, th \, y_{bj}, & \text{if } s = 0 \end{cases} \tag{23}$$

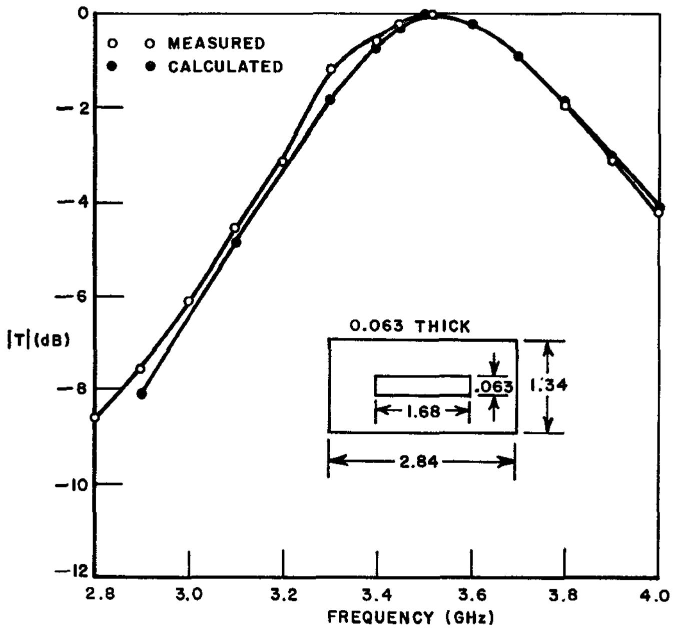

Fig. 2. Calculated and measured values of the transmission coefficient for a 0.063-in-thick rectangular slot in a waveguide versus frequency.

$$\int_b \boldsymbol{e}_{bj} \times \boldsymbol{h}_{ai} \cdot \boldsymbol{u}_z \, ds = y_{ai} \int_{(w-t)/2}^{(w+t)/2} \int_{(v-h)/2}^{(v+h)/2} \sin \left(r\pi \cdot \frac{2y - w + t}{2t} \right) \cdot \sin \left(\frac{p\pi y}{w} \right) \cdot \cos \left(s\pi \cdot \frac{2x - v + h}{2h} \right) \cdot \cos \left(\frac{q\pi x}{v} \right) dx \, dy$$

$$= y_{ai} \left\{ \frac{\cos \left[\frac{\pi}{2} (r - p) \right]}{\pi \left[\frac{r}{t} - \frac{p}{w} \right]} \cdot \sin \left[\frac{\pi}{2} \left(r - \frac{pt}{w} \right) \right] - \frac{\cos \left[\frac{\pi}{2} (r + p) \right]}{\pi \left[\frac{r}{t} + \frac{p}{w} \right]} \sin \left[\frac{\pi}{2} \left(r + \frac{pt}{w} \right) \right] \right\} \cdot \left\{ \frac{\cos \left[\frac{\pi}{2} (s + q) \right]}{\pi \left[\frac{s}{h} + \frac{q}{v} \right]} \sin \left[\frac{\pi}{2} \left(s + \frac{qh}{v} \right) \right] + \frac{\cos \left[\frac{\pi}{2} (s - q) \right]}{\pi \left[\frac{s}{h} - \frac{q}{v} \right]} \sin \left[\frac{\pi}{2} \left(s - \frac{qh}{v} \right) \right] \right\}. \tag{24}$$

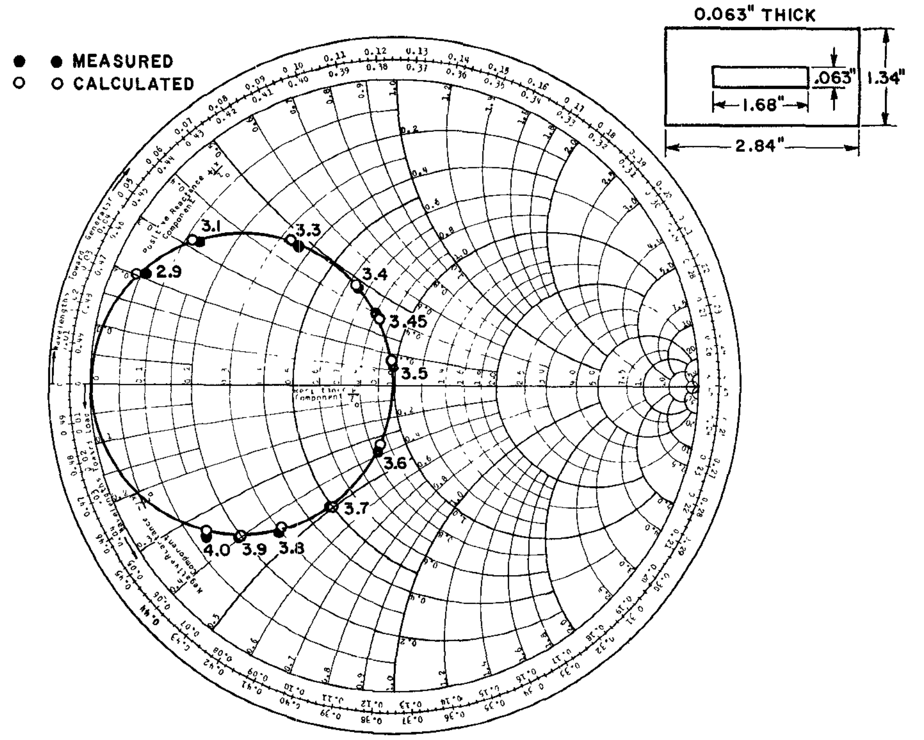

Fig. 3. Calculated and measured values of the equivalent impedance Z_{eq} for a 0.063-in-thick rectangular slot in a waveguide versus frequency.

The results in (22)–(24) are substituted into (20) and (21) when making calculations.

By solving the system of equations [i.e., (20) and (21)] for ρ, using both symmetric and antisymmetric excitation and the appropriate equation [i.e., (11) or (12)], equivalent-T circuit parameters are determined. It is now a simple matter to calculate the reflection and transmission coefficients.

The transmission coefficient versus frequency for an actual window, as measured with a slotted line, is shown in Fig. 2. Also shown is the same data calculated using the above procedure. The agreement is very good. In order to compare the calculated phase information with measured data, we show in Fig. 3 calculated and measured values of the normalized equivalent impedance Z_{eq} at the front of the window (i.e., at junction 1). A unit impedance transmission line terminated with this normalized impedance Z_{eq} has the same reflection coefficient as the waveguide containing the rectangular window, providing the window is backed by a matched load. Again good agreement is obtained between the calculated and measured values.

The data in Figs. 2 and 3 were calculated using 6 modes in the window and 120 modes in the waveguide. However, the number of modes used to approximate the fields did not appear to be critical. Values for the equivalent circuit parameters agreed to within a few percent when the number of modes in waveguide b was varied from 6 to 9, and when the number of modes in guide a was varied from 100 to 120. Since such good agreement was obtained between the calculated and measured values, there seemed to be no doubt that convergence was obtained.

The calculations were made using an IBM 360/75 computer. The simultaneous equations were solved using IBM software modified to handle complex arithmetic.

Finite Conductivity

For thin windows, the agreement between measured and calculated values of the equivalent impedance Z_{eq} at the window was excellent, as shown in the previous section. However, the thickest window that was measured ($l > \lambda$) did not show such good agreement between measurements and calculations using the modal analysis method as described previously. The calculations predicted perfect transmission at resonance, whereas the measurements showed an appreciable transmission loss. One source of loss might be the currents flowing on the metal containing the window (i.e., the hatched area in Fig. 1). One would expect the currents flowing on this surface to be relatively independent of the window thickness (i.e., the l dimension). Since windows up to 3/16 in thick did not have appreciable transmission loss, it was felt that this loss mechanism was relatively unimportant. Thus the most significant source of heat loss was felt to be the currents flowing on the waveguide walls.

Using a perturbational method, Harrington [5] gives the attenuation constant due to imperfectly conducting guide walls as

$$\alpha = \frac{R}{h\eta\sqrt{1 - (f_c/f)^2}}\left[1 + \frac{2h}{t}(f_c/f)^2\right] \qquad (25)$$

where R is the surface resistance, $\eta = \sqrt{\mu/\epsilon}$), f_c is the cutoff frequency of the waveguide, and t and h are shown in Fig. 1. The waveguide of region a is operated well above cutoff, so that very little attenuation occurs. However, for a narrow

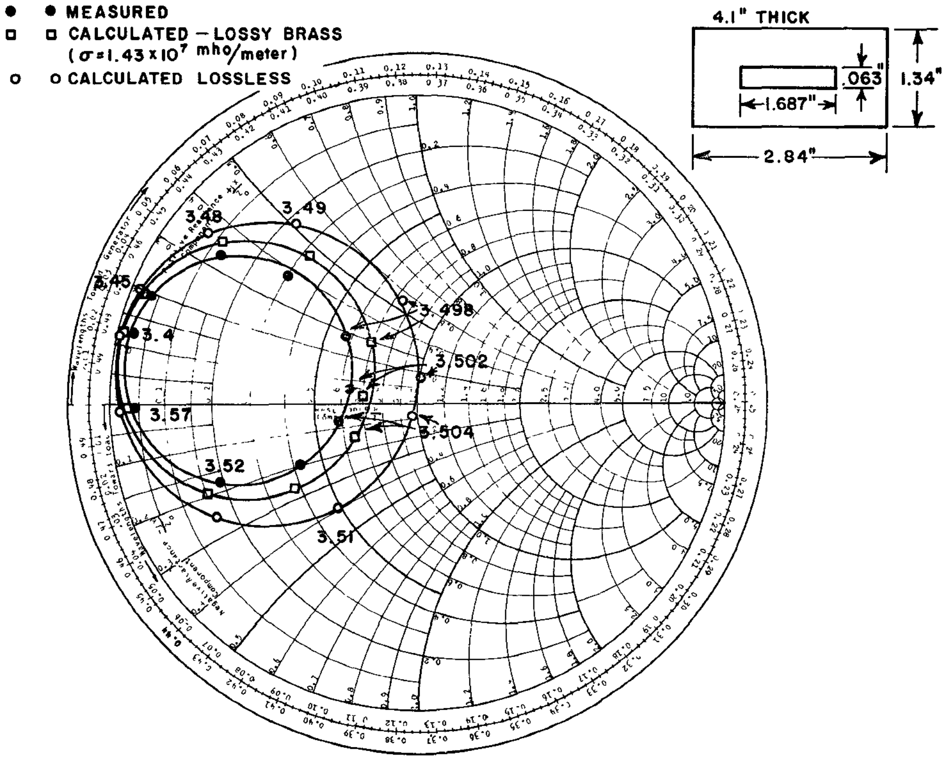

Fig. 4. Calculated and measured values of the equivalent impedance Z_{eq} for a 4.1-in-thick rectangular slot in a waveguide versus frequency. Calculated values for both a lossless slot and a slot with finite conductivity are shown.

(i.e., $h \ll \lambda$) window at resonance, $t \approx \lambda/2$, so that resonance occurs at approximately the cutoff frequency of waveguide b (i.e., the window), and $f \approx f_c$. Note that for $f = f_c$, (25) predicts $\alpha \to \infty$. Obviously, this simple perturbational approach to finite conductivity of the waveguide is not valid near cutoff. However, it serves to indicate that the finite conductivity of the window will have a definite effect on the transmission properties of a thick window.

In order to account for the effects of finite conductivity of the window near cutoff, one must consider not only the wall losses, but also the mode coupling due to the surface currents. Collin [4, p. 193] gives equations that contain the propagation constant γ as a function of the TE and TM mode coupling due to finite conductivity. Since the slots were narrow ($h \ll \lambda$), TE_{r0} modes were adequate to approximate the fields in the slot, and for TE_{r0} modes, the equations can be solved for γ. Substituting the correct values for the mode numbers, we obtain

$$\frac{(\gamma_j^2 - \Gamma_j^2)\sqrt{-1}\,\omega\mu t h}{2Z_m} + \left[\left(\frac{r\pi}{t}\right)^2 - \left(\frac{2\pi}{\lambda}\right)^2\right](2h + t) - \frac{\Gamma_j^2}{\left[\left(\frac{r\pi}{t}\right)^2 - \left(\frac{2\pi}{\lambda}\right)^2\right]} \cdot \frac{r^2\pi^2}{t} = 0. \tag{26}$$

Solving for γ_j^2

$$\gamma_j^2 = \frac{-2Z_m}{j\omega\mu}\left[r^2\pi^2 \cdot \frac{2}{t^3} + \frac{4\pi^2}{h\lambda^2}\right] + \Gamma_j^2 \tag{27}$$

where λ is the free space wavelength and Z_m is the surface impedance of the metal containing the window, and is given by

$$Z_m = \left(\frac{\omega\mu}{2\sigma}\right)^{1/2}(1 + \sqrt{-1}) \tag{28}$$

where σ is the conductivity of the metal. Note that for infinite conductivity, (27) reduces to $\gamma_j^2 = \Gamma_j^2$, as expected. Using (27) to obtain γ_j, the scattering coefficient becomes

$$S_{jj} = \pm e^{-\gamma_j l}. \tag{29}$$

The modes for waveguide b as given in (4)–(6) are no longer correct, since they were derived for perfectly conducting walls. One can approximate the modes in the lossy waveguide by assuming that the shape of the waveguide modes, i.e., their sine–cosine dependence, remains unchanged, but the wave admittance or ratio of H_y to E_x is changed. Using this approximation, we have

$$y_{b_j} = \sqrt{-1}\sqrt{\frac{\epsilon}{\mu}}\,\frac{\lambda}{2\pi}\left[\left(\frac{2\pi}{\lambda}\right)^2 - \left(\frac{r\pi}{t}\right)^2\right] \Big/ \gamma_j. \tag{30}$$

Calculations of reflection and transmission coefficients for narrow lossy windows were made using the previously described modal analysis method, except that (29) and (30) were substituted for (9) and (6), respectively. The accuracy of these calculations is illustrated in Fig. 4, where normalized values of Z_{eq} versus frequency are shown for a 4.1-in-thick brass slot. The improvement in the accuracy of the modal analysis solution obtained by including the mode-coupling

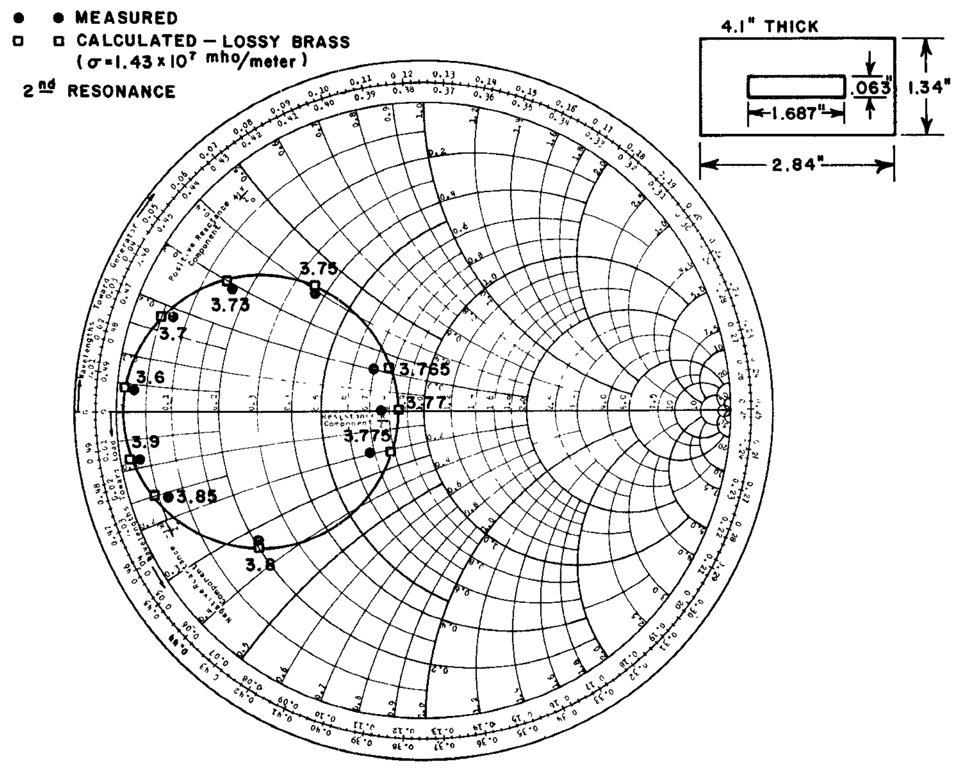

Fig. 5. Calculated and measured values of the equivalent impedance Z_{eq} for a 4.1-in-thick rectangular slot in a waveguide versus frequency. This is a continuation of Fig. 4, and shows the second resonance.

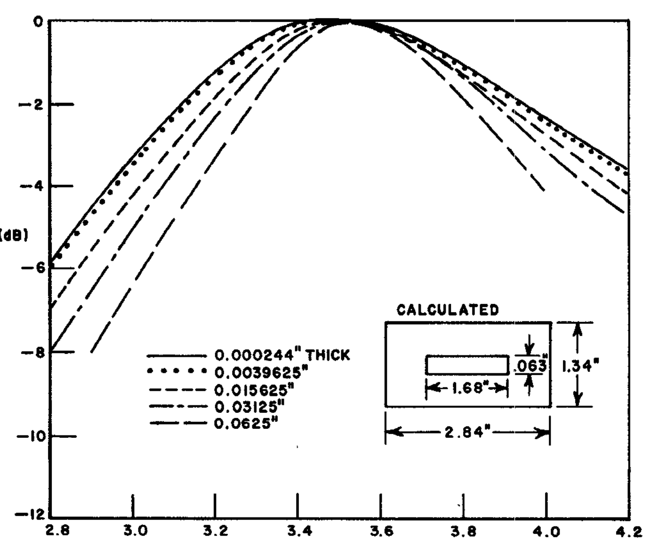

Fig. 6. Calculated values of the transmission coefficient versus frequency for thin rectangular slots in a waveguide.

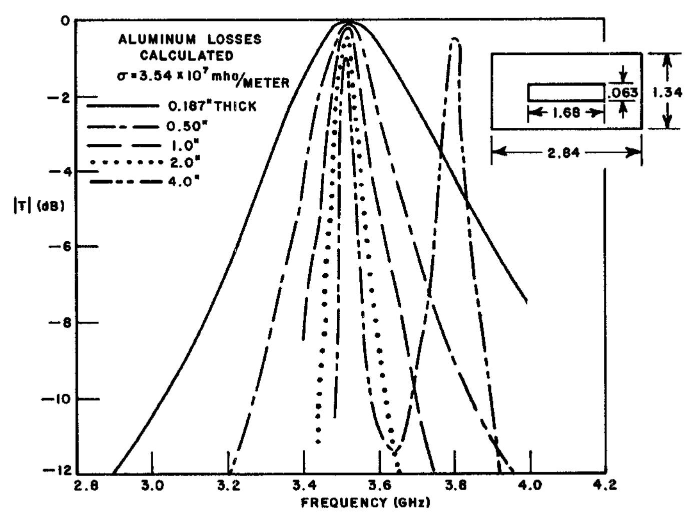

Fig. 7. Calculated values of the transmission coefficient for thick lossy aluminum slots versus frequency.

effects of finite conductivity is evident. This 4.1-in-thick slot has a second resonance in S-band. Measured and calculated values of Z_{eq} for frequencies near this resonance are shown in Fig. 5. Again the agreement is excellent.

In Figs. 6 and 7 we show curves of $|T|$ versus frequency for a 0.063- × 1.68-in aluminum waveguide window for thicknesses varying from 0.000244 to 4.0 in. For the thin slots shown in Fig. 6, the computed curves converge toward the limiting value for an infinitesimally thin window. As the slots are made thicker, the bandwidth decreases, loss increases, and multiple resonances occur, as shown in Fig. 7.

Calculated transmission curves for somewhat wider slots are shown in Figs. 8 and 9. Since these slots are wider, fewer modes were required to approximate the fields in the large waveguide. Convergence tests were made, and again the number of modes required for convergence was not critical.

The multiple resonances for thicker slots are clearly shown

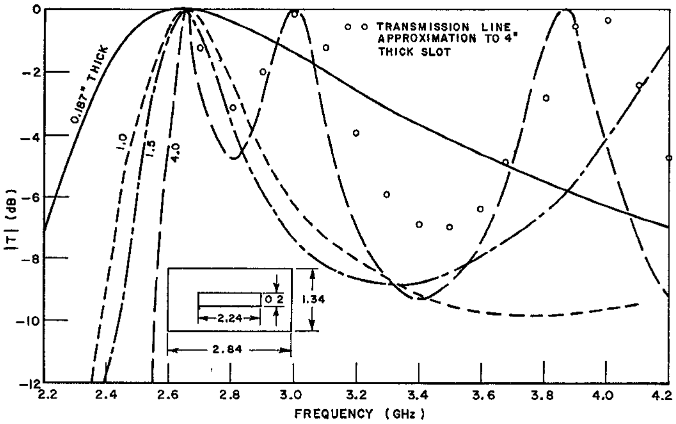

Fig. 8. Calculated values of the transmission coefficient versus frequency for 0.2-in-wide rectangular slots of various thicknesses in a waveguide.

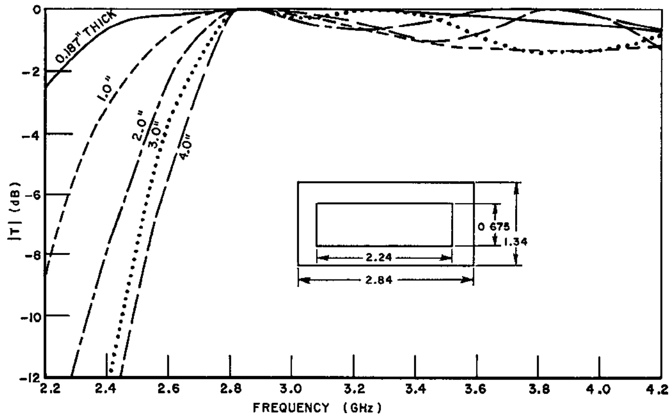

Fig. 9. Calculated values of the transmission coefficient versus frequency of 0.675-in-wide rectangular slots of various thicknesses in a waveguide.

in Fig. 8. For thick slots ($l > \lambda$), simple transmission line calculations can yield reasonably accurate results. The transmission line calculations shown in Fig. 8 were made by using the TE_{10} mode characteristic impedances [6] and neglecting the higher order modes at junctions 1 and 2.

It is evident that the slot shown in Fig. 9, if filled with dielectric to lower its cutoff frequency, would have the expected transmission characteristics of a waveguide pressure window.

Conclusions

The modal analysis method of Wexler can be used to calculate the reflection and transmission properties of thick rectangular waveguide windows. However, for thick, finitely conducting waveguide windows, the method loses accuracy because of mode coupling due to surface resistance. By modifying the modal propagation constants so as to include these effects, significant improvement in accuracy is obtained. This same technique can no doubt be used to more accurately treat other finitely conducting waveguide obstacles.

Acknowledgment

The authors wish to thank Prof. L. Peters, Jr., for the many helpful suggestions that he made concerning this work.

References

[1] L. Lewin, *Advanced Theory of Waveguides.* New York: Iliffe, 1951, pp. 21, 88–97.
[2] N. Marcuvitz, *Waveguide Handbook.* New York: McGraw-Hill, 1951, pp. 248–257, 404–408.
[3] A. Wexler, "Solution of waveguide discontinuities by modal analysis," *IEEE Trans. Microwave Theory Tech.*, vol. MTT-15, pp. 508–517, Sept. 1967.
[4] R. E. Collin, *Field Theory of Guided Waves.* New York: McGraw-Hill, 1960, pp. 193, 230.
[5] R. F. Harrington, *Time-Harmonic Electromagnetic Fields.* New York: McGraw-Hill., 1961, p. 73.
[6] E. C. Jordan and K. G. Balmain, *Electromagnetic Waves and Radiating Systems.* Englewood Cliffs, N. J.: Prentice-Hall, 1968, p. 264.

Negative TEO–Diode Conductance by Transient Measurement and Computer Simulation

HANS L. HARTNAGEL AND MITSUO KAWASHIMA

Abstract—A new method based on slow microwave transients due to steep bias-voltage steps gives a detailed negative-device-conductance function versus microwave-voltage amplitude v_{ac} for Gunn diodes. Measurements of GaAs and InP devices made by different fabrication processes as used by a variety of manufacturers show that basic differences in behavior exist. Some of these are representative of high switching speeds and others of good steady-state efficiencies. Computer simulation of Gunn devices with a range of mobility and ionized-donor density profiles oscillating in a suitable resonant structure leads to similar differences in negative-conductance functions. A first correlation between experimental and theoretical behavior is attempted, and it is possible to estimate the mobility and carrier-density profiles which could most likely be responsible for a certain device behavior.

It is shown that an external locking signal affects the device's negative conductance only for small values of v_{ac}, and experimental results confirm that this, in accordance with theoretical expectation, increases the switching speed only of certain types of diodes.

Manuscript received November 16, 1973; revised January 21, 1973. This work was supported by the Science Research Council.

The authors are with the Department of Electrical and Electronic Engineering, University of Newcastle upon Tyne, Newcastle upon Tyne, England.